

Electrogenerated chemiluminescence. 75. Electrochemistry and ECL of 9,10-bis(2-naphthyl)anthracene

Weidong Cao, Xiaohong Zhang¹, Allen J. Bard^{*}

Department of Chemistry and Biochemistry, The University of Texas at Austin, 1 University Station A5300, Austin, TX 78712-0615, USA

Received 19 September 2003; received in revised form 18 November 2003; accepted 26 November 2003

Abstract

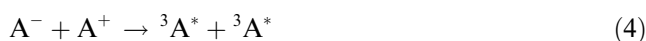
The spectroscopy, electrochemistry, and electrogenerated chemiluminescence (ECL) of 9,10-bis(2-naphthyl)anthracene (BNA) was investigated. BNA shows high fluorescence quantum yields ($\phi = 0.86$). Strong, intense ECL was observed on the surface of a Pt electrode in benzene + acetonitrile (1:1) while pulsing between the potentials for the first oxidation and reduction of BNA. The peak of ECL light emission was at 430 nm with an ECL efficiency about 90% of that of 9,10-diphenylanthracene (DPA). Cyclic voltammograms (CVs) of BNA show nernstian one-electron oxidations and reductions to the radical ions attributed to electron transfers to the anthracene core. The first reduction is followed by a second irreversible one-electron step and then two, closely spaced nernstian one-electron reductions assigned to electron transfer to the naphthalene moieties. The reduction CV was digitally simulated to establish the reduction mechanism.

© 2003 Elsevier B.V. All rights reserved.

Keywords: Chemiluminescence; Voltammograms; BNA

1. Introduction

Electrogenerated chemiluminescence (ECL) is light emission from chemical reactions between species generated by electrolysis at an electrode surface. Typical ECL is produced from the annihilation reaction of a radical anion and radical cation of a compound that are generated at the surface of an electrode by alternate pulsing of potential between the reduction and oxidation potentials. This can be represented as



In an energy-sufficient system (i.e., the enthalpy of reaction 3 is greater than the singlet excitation energy), the excited singlet state species can be directly generated from (3), which is called an “S-route”. However, in an energy-deficient system, the excited singlet is produced from triplet–triplet reaction (5) and is called the “T-route”. The T-route may occur in an energy-sufficient system as well. ECL has been applied in the area of immunoassay and DNA probes with high sensitivity and low backgrounds and in the search for new, highly efficient and stable electroluminescent compounds for potential use in organic light-emitting devices (OLEDs) [1].

BNA and its polymers, known to be new emitting materials in OLEDs and light-emitting devices (LEDs), have proved to generate efficient and stable blue light emission with low turn-on voltages [2–5]. Here, we report the spectroscopic and electrochemical characterization of BNA as well as ECL resulting from the annihilation of the radical anion $BNA^{\cdot-}$ and radical cation $BNA^{\cdot+}$ of BNA. In addition, digital simulation of the cyclic voltammogram (CV) of BNA was carried out to establish the reduction mechanism of BNA.

^{*} Corresponding author. Tel.: +1-5124713761; fax: +1-5124710088.

E-mail address: ajbard@mail.utexas.edu (A.J. Bard).

¹ Technical Institute of Physics and Chemistry, Chinese Academy of Sciences.

2. Experimental

2.1. Materials

BNA was synthesized according to published procedures [6]. Anthracene (AN) and 9,10-diphenylanthracene (DPA), purchased from Sigma, were used as received. The supporting electrolyte, tetra-*n*-butylammonium hexafluorophosphate (TBAPF₆) was recrystallized twice from EtOH+H₂O (4:1) and dried in a vacuum oven at 100 °C prior to being transferred into an inert atmosphere dry box (Vacuum Atmosphere, Hawthorne, CA). Anhydrous benzene (Aldrich, ACS spectrophotometric grade) and anhydrous acetonitrile (Aldrich, biotech grade) were used as received. All solutions for measurements outside the dry box were prepared in the dry box and sealed in airtight vessels.

A platinum disk electrode (2.2 mm diameter) was employed as the working electrode with a Pt wire as the auxiliary electrode and a silver wire as the quasi-reference electrode (QRE). The potential of the QRE was calibrated with respect to the ferrocene/ferrocenium (Fc/Fc⁺) couple (taking $E_{\text{Fc}/\text{Fc}^+}^0 = 0.424$ V vs. SCE). The working electrode was polished on a belt pad with 0.05 μm alumina powder (Buehler, Lake Bluff, IL) and sonicated in water and ethanol for 2 min, and then dried in a vacuum oven at 100 °C before being transferred into an inert atmosphere dry box.

2.2. Instrumentation

Cyclic voltammograms were recorded on a CH Instruments Electrochemical Work Station (CH Instruments, Austin, TX). All ECL measurements were performed as previously reported [7] utilizing a charged coupled device (CCD) camera (Photometrics CH260, Photometrics-Roper Scientific, Tucson, AZ), which was cooled to -103 °C during the experiment. The CCD camera and grating (American Holographic (Littleton, MA), Model No. 100S) were calibrated with a mercury lamp prior to each measurement. Integration times for measurement of the ECL spectra were 2 min. All fluorescence spectra were measured on a QuantaMaster PTI Fluorometer (Photo Technology International) using a slit width of 1 nm and a resolution of 1 nm. All the UV-

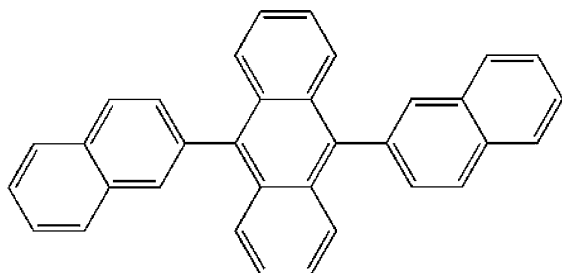


Fig. 1. Molecular structure of BNA.

visible spectra were measured on a Milton Roy Spectronic 3000 array spectrophotometer. Digital simulation was performed using DigiSim 3.0 for Windows (Bioanalytical Systems).

3. Results and discussion

3.1. Electrochemistry of BNA

A CV of BNA in benzene + acetonitrile (1:1) solution with 0.1 M TBAPF₆ as supporting electrolyte is shown in Fig. 2, along with those of AN and DPA for comparison. The oxidation of BNA was characterized by two redox peaks observed at the potentials of 1.22 and 1.79 V vs SCE. The height of the first wave was con-

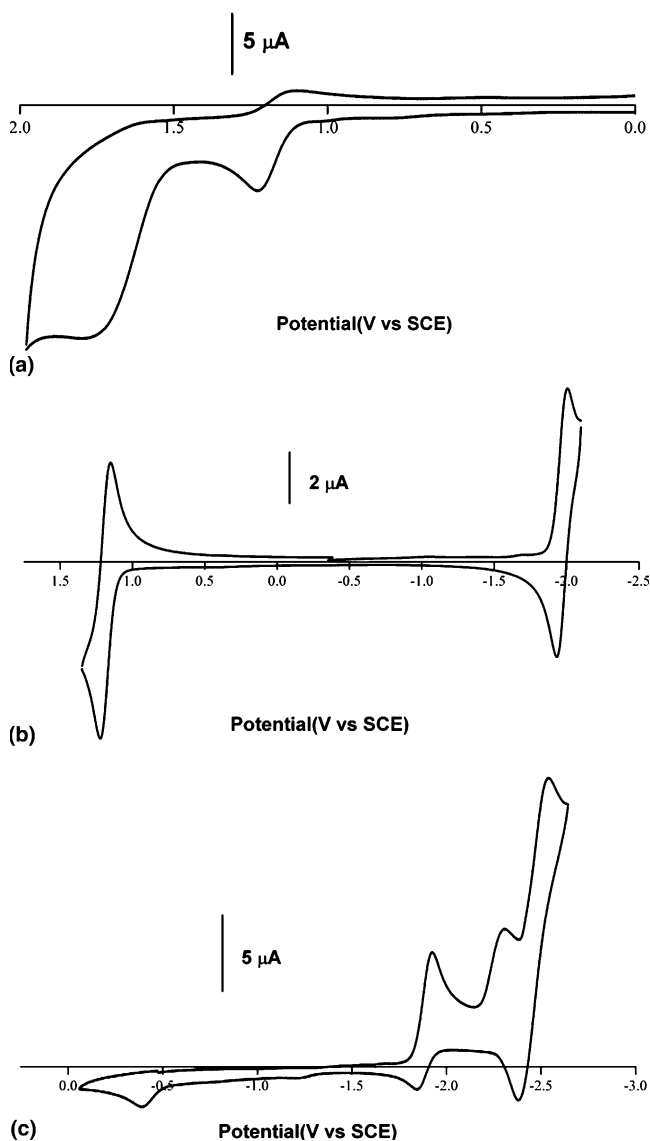


Fig. 2. CVs of 10 mM of BNA in 0.1 M TBAPF₆ in benzene + acetonitrile solution (1:1) at a platinum electrode (scan rate, 0.1 V/s). Note that the cathodic current is plotted positive upwards.

sistent with one-electron transfer by comparison with DPA and corresponded to the formation of the radical cation. The value of I_{pa}/I_{pc} was unity over a range of scan rate of 0.01–0.2 V/s, indicating a chemically reversible one-electron transfer at the potential of 1.22 V. That I_{pa} and I_{pc} were proportional to $v^{1/2}$ indicates diffusion control in this process and stability of the radical cation. The naphthyl substituent groups at the 9 and 10 positions of AN lead to a decrease of oxidation potential by about 50 and 10 mV when compared to AN and DPA. The investigation of electrochemistry and electron spin resonance spectroscopy of 9,10-di(1-naphthyl)anthracene, which has a similar molecular structure to BNA, indicated that the second broad irreversible oxidation wave observed at the potential of 1.79 V vs SCE corresponds to the formation of the highly reactive radical dication [8]. The irreversibility of the second wave is probably due to a following chemical reaction of product with solvent, electrolyte, or trace water in the system (see Fig. 1).

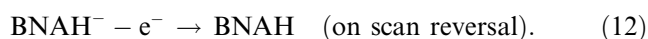
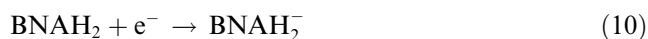
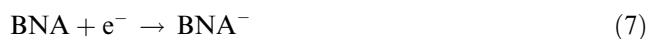
The reduction of BNA in benzene + acetonitrile (1:1) solution containing 0.1 M TBAPF₆ is shown in Fig. 2(c). Three reduction waves were observed when the potential was scanned in the negative direction. The first reduction wave of BNA appeared at –1.92 V vs SCE. The peak height of the first reduction wave was essentially the same as the first oxidation wave, consistent with one-electron transfer, and corresponds to the formation of the radical anion. The peak-to-peak potential separation, ΔE_p , was 67 mV, about the same as the Fc/Fc⁺ couple in this medium, so the difference from 60 mV represents uncompensated IR and the wave can be considered nernstian. The I_{pa} and I_{pc} values proportional to $v^{1/2}$ for v from 0.01 to 0.2 V/s, indicate a diffusion controlled process. Additionally, the value of I_{pc}/I_{pa} was found to be unity indicating no following chemical reaction. These results indicate the formation of a stable radical anion. Compared to AN and DPA, the reduction potential of BNA shifted positively by 140 and 60 mV, respectively.

The second reduction wave at –2.30 V vs SCE was an irreversible process. This is probably the formation of the dianion on the AN moiety, as found with AN and DPA. This species is sufficiently basic to abstract protons from MeCN or trace water in the system. This protonation reaction is very fast and no reversal wave was seen for v up to 10 V/s.

The third larger broad reduction wave at –2.54 V vs SCE showed a ΔE_p of about 160 mV. The peak height of this wave was about twice that of the second reduction wave, which is indicative of a two-electron transfer process, probably occurring on the two naphthyl substituent groups on BNA molecule. After traversing this wave and then scanning in the positive direction, an irreversible oxidation wave at about –0.433 V vs SCE was observed. The same oxidation wave was found if re-

versal was carried out after only the second reduction wave and suggests this is the oxidation of the protonated dianion of BNA.

Based on the above results, the assumed mechanism of the reduction of BNA in benzene + acetonitrile (1:1) solution containing 0.1 M TBAPF₆ is outlined in the following equations:



While scanning in the positive direction, BNAH[–] (or perhaps BNAH₂), the product of the 2e[–] reduction of BNA, was oxidized with the half-wave potential of 0.43 V vs SCE in an irreversible process.

Digital simulation of the CV for the reduction of BNA discussed above was performed. The experimental voltammogram of 1.0 mM of BNA in benzene + acetonitrile (1:1) solution containing 0.1 M of TBAPF₆ at $v = 0.1$ V/s was used for comparison to the results of the simulation. During the simulation, all the electron-transfer reactions were considered fast ($k_0 = 1 \times 10^5 \text{ s}^{-1}$) and α values were taken to be 0.5. Diffusion coefficients for all compounds were assigned as $1.0 \times 10^{-5} \text{ cm}^2/\text{s}$. The equilibrium constant for the dianion protonation reaction, taken as a pseudo first-order reaction, was set to a high value ($k_{eq} = 1.0 \times 10^{12}$). The ratio of the rate of protonation reaction to scan rate ($k_f v$) is an important factor influencing peak current and peak potential [9]. When $k_f v$ was set to a value lower than 1.0×10^4 , an anodic current corresponding to oxidation of BNA^{2–} appeared in the simulated voltammogram. When k_f was $>1.0 \times 10^6$, this anodic current disappeared and the profile of the voltammogram was more consistent with the experimental voltammogram. However, a higher value of $k_f v$ leads to a larger shift in the peak potential of the second reduction wave. By setting the E^0 of the second reduction wave –2.28 and –2.37 V, basically the same simulated voltammograms were obtained with $k_f v$ values of 1.0×10^7 and 1.0×10^{10} , respectively. Therefore, it is difficult to determine the standard reduction potential when k_f and the heterogeneous electron transfer rate constants are unknown. For the two-electron transfer reaction corresponding to the third reduction wave, ΔE^0 of the two-electron transfer steps depends on the extent of interaction of the naphthyl groups across the AN center [10]. Assuming ΔE^0 between the two-electron transfers is 42 mV, we obtain the simulated CV shown in Fig. 3. The theoretical and

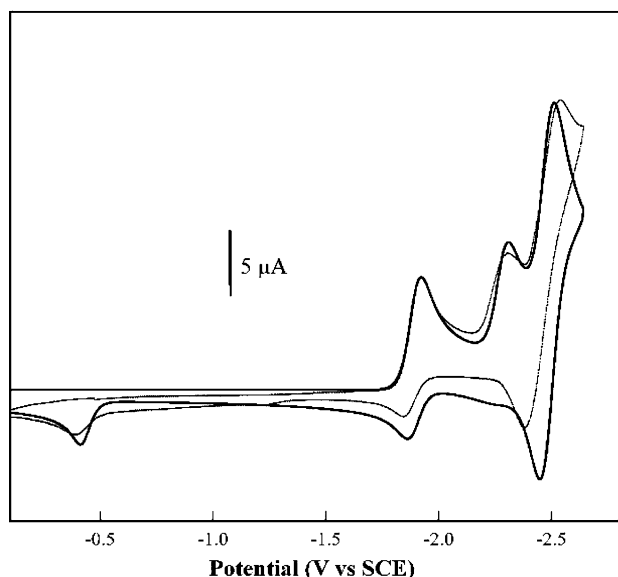


Fig. 3. Comparison of simulated (—) and experimental (---) CVs of 1.0 mM BNA in 0.1 M TBAPF₆ in benzene + acetonitrile solution (1:1) with a scan rate of 0.1 V/s. Simulation conditions: $k_{\text{eq}} = 1 \times 10^{12}$, $k_{\text{f}} = 1 \times 10^6$, $k_{\text{s}} = 1 \times 10^4$, $E_1^0 = -1.822$ V, $E_2^0 = -2.28$ V, $E_3^0 = -2.39$ V, $E_4^0 = -2.432$ V, $E_5^0 = -0.43$ V vs SCE, scan rate was 0.1 V/s and a semi-infinite mechanism was used in simulation.

experimental voltammograms match pretty well except at the third reduction wave, where the peak splitting, ΔE_{p} , for the simulation was 63 mV compared to the experimental result (which probably contains considerable IR-drop) of 130 mV. The last experimental reduction wave was also perturbed by the large background current for the reduction of the solvent/electrolyte.

3.2. Electrogenerated chemiluminescence

The absorption and fluorescence spectra for BNA in benzene + acetonitrile (1:1) solution are shown in Fig. 4.

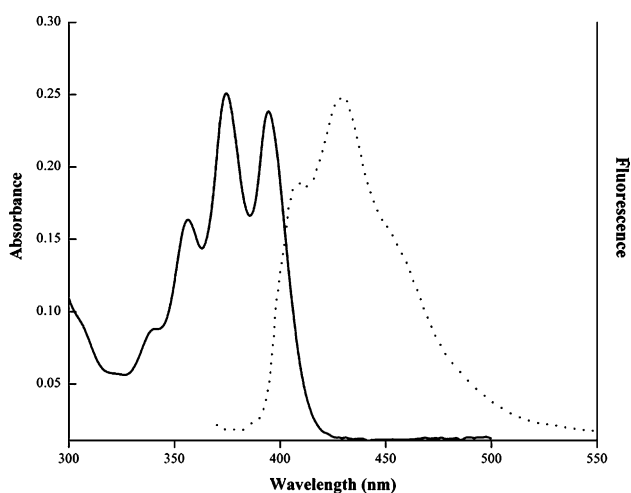


Fig. 4. Optical absorption (—) and fluorescence spectra (···) of 2.0 μM of BNA in benzene + acetonitrile (1:1) solution (1 cm path length; $\lambda_{\text{exc}} = 375$ nm).

As shown, BNA shows two strong absorption peaks at 375 and 395 nm, which are attributed to transitions in the AN moiety. The molar extinction coefficient of BNA was $12,680 \text{ M}^{-1} \text{ cm}^{-1}$ at 375 nm. The absorption and fluorescence spectra for AN and DPA were measured under the same experimental conditions for comparison. 19 and 2 nm red shifts in BNA absorption band were observed compared to those of AN and DPA, respectively. The fluorescence maximum of BNA in benzene + acetonitrile was at 422 nm. Using DPA as the standard, the quantum efficiency of BNA was 0.86. Compared to AN and DPA, the maximum emission peaks of BNA were red-shifted by 20 and 12 nm, respectively. This indicates the effect of naphthyl groups at the 9 and 10 positions and shows some delocalization, and hence some interaction between the naphthyl groups. However, because of steric interactions, the naphthyl groups are expected to lie largely outside of the plane of the AN.

Alternately pulsing between the first oxidation peak potential of BNA, 1.22 V vs SCE, and the first reduction peak potential, -1.92 V vs SCE, resulted in a bright blue light emission from the surface of the working electrode. The intensity of light emission was so strong that it could be observed with the naked eye in a darkened room. The ECL spectrum of BNA in benzene + acetonitrile (1:1) solution with 0.1 M TBAPF₆ as supporting electrolyte is shown in Fig. 5. The ECL emission band of BNA shows a maximum emission at 430 nm. Compared to the fluorescence spectrum, the ECL spectrum appears slightly broader in shape, mainly because the slit used in the ECL measurement was much larger than that in the

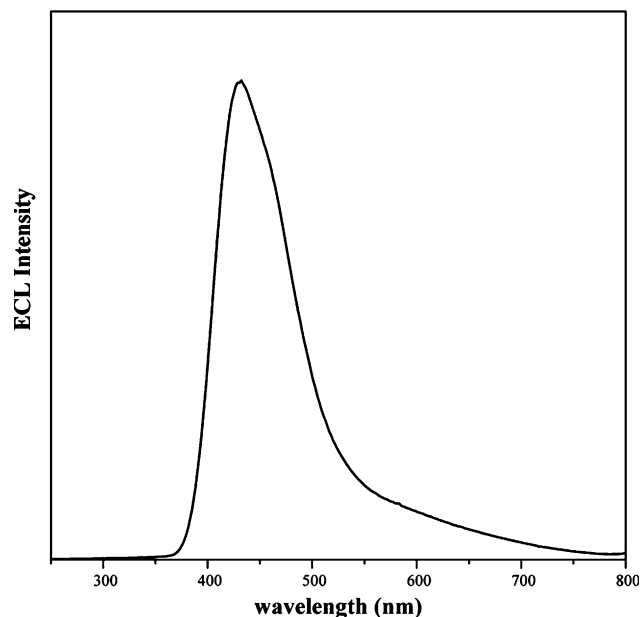


Fig. 5. ECL of 1.0 mM of BNA in benzene + acetonitrile (1:1) with 0.1 M TBAPF₆ as supporting electrolyte. (10 Hz pulsing between 1.22 V and -1.92 V vs SCE.)

fluorescence measurement, with, at most, a 6 nm red shift. The light emission was very stable in the first 2 min. It then gradually decayed and lasted about 30 min. A comparison of the CVs from before and after this ECL decay experiment showed only a slight decrease of I_{pc} and I_{pa} of the reduction of BNA. Similar behavior has been seen earlier for many other organic ECL systems, where decay of the ECL occurs without appreciable loss of the ECL active species [1]. This suggests that the decay in ECL is caused by the build up of a quencher. The small instability might be the result of a small amount of disproportionation of the radical ions to produce unstable dications or dianions.

The total Gibbs energy of the above annihilation reaction ($\Delta H_{ann} = \Delta G_{ann} + T\Delta S$), equal to the difference between pulse potentials ($\Delta E_{p(ox/red)} \sim 3.1$ eV) subtracting entropy effects (~ 0.1 eV), yields 3.0 eV, which is sufficient to produce the singlet-excited state directly (2.93 eV). The ECL efficiency for the BNA annihilation was about 90% of DPA under the same conditions, indicating that the ECL of BNA is a highly efficient process.

4. Conclusions

The photochemistry, electrochemistry, and electro-generated chemiluminescence (ECL) of 9,10-bis(2-naphthyl)anthracene (BNA) was investigated. Influenced by naphthyl groups at the 9 and 10 positions, the absorption peaks are shifted to the red by 19 and 2 nm, and the fluorescence peaks are shifted to the red by 20 and 12 nm when compared to those of AN and DPA. The fluores-

cence quantum yield was 0.86. Strong blue ECL emission was observed from a BNA solution with an emission peak at 430 nm and the ECL efficiency was 90% of that for DPA. The mechanism of reduction was proposed to involve first and second electron transfers on the anthracene (AN) center followed by a fast protonation reaction. The third and fourth electron transfers occurred on the two naphthyl groups.

Acknowledgements

The support of this research by the Robert A. Welch Foundation and IGEN International Inc. is gratefully acknowledged.

References

- [1] A.J. Bard, *Electrogenerated Chemiluminescence*, Marcel Dekker, New York, 2004 (in press).
- [2] S. Zheng, J. Shi, *Chem. Mater.* 13 (2001) 4405.
- [3] Y. Li, M.K. Fung, Z. Xie, S.-T. Lee, L.S. Hung, J. Shi, *Adv. Meter.* 14 (2002) 1317.
- [4] X.H. Zhang, M.W. Liu, O.Y. Wong, C.S. Lee, H.L. Kwong, S.T. Lee, S.K. Wu, *Chem. Phys. Lett.* 369 (2003) 478.
- [5] J.M. Shi, C.H. Chen, K.P. Klubek, US Patent 5974247 (2000).
- [6] N. Miyaura, A. Suzuki, *Chem. Rev.* 95 (1995) 2457.
- [7] P. McCord, A.J. Bard, *J. Electroanal. Chem.* 318 (1991) 91.
- [8] L.S. Marcoux, A. Lomax, A.J. Bard, *J. Am. Chem. Soc.* 92 (1970) 243.
- [9] A.W. Bott, *Curr. Separ.* 18 (1999) 9.
- [10] A.J. Bard, L.R. Faulkner, *Electrochemical Methods*, Wiley, New York, 2001, p. 505.